Talanta 97 (2012) 157–162

Contents lists available at SciVerse ScienceDirect

Talanta

journal homepage: www.elsevier.com/locate/talanta

Reagentless and calibrationless silicate measurement in oceanic waters

William Giraud [a,1], Ludovic Lesven [b,1], Justyna Jońca [a], Carole Barus [a], Margaux Gourdal [a], Danièle Thouron [a], Véronique Garçon [a,*], Maurice Comtat [c]

[a] Laboratoire d'Etudes en Géophysique et Océanographie Spatiales, Centre National de la Recherche Scientifique, UMR CNRS 5566, 18 Avenue Edouard Belin, 31401 Toulouse Cedex 9, France
[b] Laboratoire Géosystèmes, UMR CNRS 8217, UFR des Sciences de la Terre, Université Lille 1, 59655 Villeneuve d'Ascq Cedex, France
[c] Laboratoire de Génie Chimique, UMR CNRS 5503, 118 route de Narbonne, 31062 Toulouse Cedex 9, France

ARTICLE INFO

Article history:
Received 10 February 2012
Received in revised form
30 March 2012
Accepted 4 April 2012
Available online 10 April 2012

Keywords:
Molybdenum
Silicate
Reagentless
Amperometry
Calibrationless

ABSTRACT

Determination of silicate concentration in seawater without addition of liquid reagents was the key prerequisite for developing an autonomous *in situ* electrochemical silicate sensor (Lacombe et al., 2007) [11]. The present challenge is to address the issue of calibrationless determination. To achieve such an objective, we chose chronoamperometry performed successively on planar microelectrode (ME) and ultramicroelectrode (UME) among the various possibilities. This analytical method allows estimating simultaneously the diffusion coefficient and the concentration of the studied species. Results obtained with ferrocyanide are in excellent agreement with values of the imposed concentration and diffusion coefficient found in the literature. For the silicate reagentless method, successive chronoamperometric measurements have been performed using a pair of gold disk electrodes for both UME and ME. Our calibrationless method was tested with different concentrations of silicate in artificial seawater from 55 to 140×10^{-6} mol L^{-1}. The average value obtained for the diffusion coefficient of the silicomolybdic complex is $2.2 \pm 0.4 \times 10^{-6}$ cm^2 s^{-1}, consistent with diffusion coefficient values of molecules in liquid media. Good results were observed when comparing known concentration of silicate with experimentally derived ones. Further work is underway to explore silicate determination within the lower range of oceanic silicate concentration, down to 0.1×10^{-6} mol L^{-1}.

1. Introduction

Orthosilicic acid $Si(OH)_4$ or silicate is a key element in the control of the carbon cycle in natural waters (oceans and rivers). The source of silicate in aquatic media is mainly due to chemical weathering of silicate minerals. The delivery of silicate by rivers is influenced by lithology, weathering intensity and diatom production [1,2]. Another process in which silicate plays a key role is anthropogenic CO_2 sequestration through the biological carbon pump. Indeed diatoms, silica-shelled unicellular algae, require silicate to build their siliceous algal skeleton [3]. The C/Si/N/P molar composition of diatoms is proposed to be 106/15/16/1 [4]. These values also represent the ratios in which nutrients containing these elements are incorporated during phytoplankton growth and are released during phytoplankton decomposition and subsequent remineralization. As fast sinking particles, diatoms play a major role in exporting organic carbon to abyssal marine sediments and thus in sequestering CO_2 [5]. So, any change in silicon concentration in a globally warming ocean can alter the distribution and abundance of diatom species. Due to regional differences in spatial distribution, silicate constitutes also an excellent tracer of water masses in the ocean. Thus long term autonomous monitoring of the silicate concentration is of utmost importance to both understand changes in the biological carbon pump and to detect any modification in spreading and mixing of water masses.

In the literature, several methods including spectrophotometry, atomic absorption spectrometry, atomic emission spectrometry and high-performance liquid chromatography (HPLC) have been proposed for the determination of silicate [6]. The determination of silicate ion can also be performed by ion exclusion chromatography, with detection by post-column reaction [7].

In oceanography, determination of silicate is usually performed with an automatic colorimeter analyzer where measurement is based on the yellow color of a silicomolybdic acid. This complex is formed when ammonium molybdate is mixed with a solution of sulfuric acid and after reduction with ascorbic acid. The resulting color may be compared with that of standard solutions by spectrophotometry [8].

Long term monitoring in marine environments requires significant progress in miniaturization and decrease in energy consumption for the *in situ* autonomous instrumentation. Electrochemistry

* Corresponding author. Tel.: +33 5 61 33 29 57; fax: +33 5 61 25 32 05.
E-mail address: veronique.garcon@legos.obs-mip.fr (V. Garçon).
[1] Co-first authors.

0039-9140/$ - see front matter © 2012 Elsevier B.V. All rights reserved.
http://dx.doi.org/10.1016/j.talanta.2012.04.011

proves to be a promising methodological avenue for fulfilling these requirements and achieving excellent figures of merit (fast response time, robustness, good reproducibility, etc.) for a silicate sensor.

The method must be simple, based on basic fluidics with no liquid reagent, no solution for calibration and the possibility of self calibration. It should involve sensitive surfaces easily cleaned, insensitive to marine corrosion and biofouling. Dissolved nutrients such as silicate and phosphate are non-electroactive compounds. The electroinactivity of these compounds involves the setting up of a chemical reaction to transform them into a complex, characterized by heterogeneous electron transfer with metallic surfaces [9–13].

A method without addition of any liquid reagent using chronoamperometry has been developed based on the simultaneous formation of the molybdenum salt and protons on the anode of a divided electrochemical cell. Voltammetric detection of silicate was shown to be feasible within the range of concentrations found in the ocean (between 0.3 and 160×10^{-6} mol L^{-1}) in about 6 min. The detection limit was 1×10^{-6} mol L^{-1} [11,12]. The objective of the work presented here is to propose a calibrationless method for the *in situ* autonomous determination of silicate concentrations. The method is based on chronoamperometric oxidation of molybdenum followed by a time delay to allow the silicomolybdic complex formation and its detection by two successive chronoamperometric measurements on different sizes electrodes. The paper is structured as follows. Section 2 presents basics of diffusion phenomena and mathematical equations applied on some electrochemical problems. From these statements a calibrationless method is proposed in Section 3. To set up the method, ferricyanide is used to check accurately the radius of the disk electrodes, ferrocyanide to validate the calibrationless method and first results are presented with silicate in artificial seawater.

2. Diffusion as mass transport for direct determination of D_0 and C

Analytical electrochemical methods are in general based on the coupling between mass transport phenomena (convection, migration, diffusion) and heterogeneous electron transfer at the interface between an electronic conductor and species in solution. Convection and migration effects are neglected due to the absence of stirring and the presence of an electrolyte support respectively, which allows considering only diffusion, mostly in semi-infinite conditions [14]. The simplest method is chronoamperometry performed at constant potential. The mathematical approach consists of resolving the second Fick's law (the initial and infinite conditions are fixed and the method allows to determine the interfacial condition). The first step of the calculation leads to concentration profiles of the electroactive species at time t. The interfacial flux is then injected in the definition of the current intensity. Table 1 (2nd column) summarizes the operations leading to the relationship between the measured intensity value and the unknown concentration C_0^*. Only equations corresponding to planar electrodes are considered here since this geometry is the simplest to perform for our application. The different equations in Table 1 involve the intensity of the current I, the diffusion coefficient D_0, the concentration at infinite C_0^*, the concentration at the surface of the electrode C_0 ($x=0$), the number of transferred electrons n, the electroactive surface of the electrode A, the electroactive radius r_0, the normal distance to the surface of the planar electrode x, the time t, the electrical charge Q and the Faraday constant F. The Cottrell's equation shows the necessity to know n, D_0 and A, some variables generally determined with a calibration performed in the same conditions than the measurement. However it appears essential to have theoretical or experimental tools to determine them.

Table 1
Main steps for the resolution of second Fick's law in semi-infinite diffusion. Chronoamperometry (constant potential) at planar electrode is considered. D_0 in $cm^2\ s^{-1}$; C_0^* and C_0 ($x=0$) in mol cm^{-3}; A in cm^2; and x in cm; t in s; Q in C and F in C mol^{-1}.

	Chronoamperometry at planar electrode
2nd Fick's law	$\frac{\partial C}{\partial t}=D_0\frac{\partial^2 C}{\partial x^2}$
Boundary conditions	$C_0\ (x,\ 0)=C_0^*$ $C_0\ (\infty,\ t)=C_0^*$ $C_0\ (0,\ t)=0\ (t>0)$
Flux $-J=\frac{I}{nFA}=D_0\left(\frac{\partial C_0}{\partial x}\right)_{x=0}$	$I=nFAD_0\left(\frac{\partial C_0}{\partial x}\right)_{x=0}$
Concentration profile C_0	$C_0=C_0^* erf\left[\frac{\partial C_0}{2(D_0t)^{1/2}}\right]$
Intensity I	*Cottrell's equation:* $I=\frac{nFAD_0C_0^*}{(\pi D_0t)^{1/2}}$
Charge Q	$Q=\frac{2nFAD_0^{1/2}C_0^*t^{1/2}}{\pi^{1/2}}$

For calibration, different strategies have been developed during decades. A direct determination of concentration has been proposed by electrical charge measurement but demanding a rigorous sample preparation [19,20]. Original methods for simultaneous determination are the use of two methods [21–23], measurements on electrodes with different forms [24,25]—planar or cylindrical [26], the use of one electrode on different timescales [27–32].

Before *in situ* measurements with the sensor, the determination of the diffusion coefficient value could be possible depending on different experimental conditions influencing its value such as conductivity or temperature. Indeed, if the *in situ* sensor in the ocean is equipped with conductivity and temperature probes, the data could be stored for an eventual correction. This estimation could be done on the lab bench using various electrochemical methods as described before. Another methodology for determining the diffusion coefficient D_0 value could be the "time of flight" [15–18]. However in order to have a more precise value and a simpler method for the determination of the diffusion coefficient, we propose here to use a direct simultaneous determination of both concentration and diffusion coefficient.

When solving second Fick's law for different geometries [14], the corresponding equation is composed of two terms, one of which is time dependent and the other is not. These two components correspond to the transient state governed by the Cottrell's equation ($I=nFAD_0C_0^*/(\pi D_0t)^{1/2}$, Table 1) and to a steady state achieved at longer times. As the current intensity is recorded *versus* time, one can easily plot I *versus* $t^{-1/2}$ for short times, the origin intercept and the slope of the linear regression curve will then give a linear system with two equations. From this system of two equations, one can select two out of the three unknowns: D_0, C_0^* and n. Original works done on these determinations were done by Lingane and Loveridge [25] and Brown [26] who proposed to determine values of n and D_0. Later, Kakihana et al. [27] used ultramicroelectrode (hereafter UME) for the accurate measurement of D_0. The development of theoretical solutions allowed Winlove et al. [28] to propose the simultaneous determination of D_0 and C_0^* of oxygen in solutions of albumin. In the early 90s, Amatore et al. [22] studied in details different possibilities among several calibrationless methods and they found good results with chronoamperometry at steady state with an UME. Denuault et al. [29] then confirmed these works. In a general manner, a calibrationless method can be set in using two electrochemical methods, the combination of which allows the

mathematical determination of both D_0 and C_0^*. Other different possibilities of sizes and geometries of electrodes can be combined for a calibrationless method: a ring UME associated with planar, cylindrical or spherical electrode or a planar electrode associated with a spherical or cylindrical electrode. More recently numerical improvements in modeling allow to foresee more complex miniaturized systems [31,32], which could be of particular interest for *in situ* measurements.

Different procedures for electrode constructions can be found in the literature in forms of rings, disks, spheres and cylinders made from materials such as gold, platinum, silver or carbon. As seen previously, the direct determination of electroactive species without calibration may require the successive measurement of current across two electrodes with different sizes or forms.

In the present study, we propose to associate a planar disk microelectrode (hereafter ME) of millimetric size and a planar disk UME of micrometric size. Both are used in semi-infinite conditions and the applied potential corresponds to the first reduction of the silicomolybdic complex [11,12]. Different mass transport regimes can be considered at planar electrodes during the measurement. For each electrode (ME and UME) and at very short times, the variation of current respects Cottrell's equation. Species present at a distance inferior to the diffusion layer from the surface of the electrode are reduced, leading to a relatively high current and creating a gradient of concentration. At relatively long experimental times, steady state is reached, governed by pure diffusional mass transport and a constant current is measured. Hemispherical diffusion brings species to the surface of the UME (Fig. 1a) while a linear diffusion, orthogonal to the surface (Fig. 1b), is observed for the ME (Fig. 1b). On the UME, with a radius r_{UME}, the resolution of the second Fick's law leads to the following term for the steady state:

$$I_{UME} = 4nFD_0C_0^*r_{UME} \quad (1)$$

Depending on the size of the electrodes and time scale of the measurement, true diffusional steady state may be altered to the benefit of natural convection. This mass transport occurs when the thickness of the diffusion layer becomes comparable to the thickness of the convective-free domain [33,34]. In this study we took care to keep our experimental conditions under a pure diffusional mass transport.

The combination of Cottrell's equation (Table 1: $I_{ME} = nFA_{ME}D_0C_0^*/(\pi D_0 t_{ME})^{1/2}$ with $A_{ME} = \pi r_{ME}^2$; t_{ME} time of application of constant potential and I_{ME} the corresponding current intensity at each time t_{ME}) and Eq. (1) leads to the calculation of D_0:

$$D_0 = \frac{\pi}{16t_{ME}}\left(\frac{I_{UME}r_{ME}^2}{I_{ME}r_{UME}}\right)^2 \quad (2)$$

Then determination of the concentration C_0^* is possible using Eq. (1) or Cottrell's equation. The theory of this calibrationless method was first checked with a well known electrochemical system, then tested in a second step in artificial seawater.

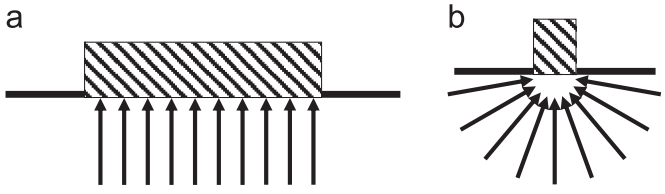

Fig. 1. Lines of diffusion field of the electroactive species arriving at the surface of a planar electrode (a) and an ultramicroelectrode (b).

3. Material and methods

3.1. Apparatus and electrodes

Amperometric measurements were carried out at room temperature (298 K) with a voltammetric analyzer comprising a PGSTAT 128N Metrohm equipped with an ECD module controlled by the GPES 4.9 software. A silver/silver chloride/KCl (3 mol L^{-1}) electrode and a platinum wire were used as the reference electrode and the auxiliary electrode, respectively. All potential values in this paper are given *versus* this Ag/AgCl/Cl^- reference electrode purchased from Metrohm. For the calibrationless method a disk ME of 1.5 mm radius (Metrohm) or 0.5 mm radius (homemade) is associated to a disk UME of 12.5 μm or 25.0 μm radii (homemade). All homemade electrodes were prepared in the laboratory from a gold wire supplied by Goodfellow and sealed into an inert and electric insulating epoxy resin. Gold for homemade electrodes, platinum and molybdenum wires were supplied by Goodfellow.

Pre-treatment—before each experiment, the gold electrode surfaces were polished with alumina oxide paper 0.3 μm and rinsed with distilled water. Finally, cyclic voltammograms were carried out in 0.5 mol L^{-1} sulfuric acid (H_2SO_4) at 100 mV s^{-1} between 0 and 1.55 V until reproducible current–potential curves were obtained.

3.2. Reagents and solutions

All solutions were prepared in Milli-Q water (Millipore Milli-Q water system) and put into polypropylene containers. Glass cannot be used as it releases silicate in solution.

Artificial seawater was prepared with sodium chloride (NaCl) supplied by Merck to obtain a salinity of 34.5 g L^{-1}.

The electroactive surface of gold is activated in 0.5 mol L^{-1} H_2SO_4 solution prepared from a 98% H_2SO_4 solution from Merck.

Trihydrated potassium ferricyanide ($K_3Fe(CN)_6 \cdot 3H_2O$) and trihydrated potassium ferrocyanide ($K_4Fe(CN)_6 \cdot 3H_2O$) were purchased from VWR Prolabo and potassium chloride (KCl) from Merck. Argon gas was used to avoid ferrocyanide oxidation.

3.3. Analytical procedures

Electroactive surface determination—chronoamperometric measurements were performed in semi-infinite diffusion conditions on each gold working electrode. Time electrolysis depends on the electrode used: a potential of 0.2 V was applied for ferricyanide reduction during 60 s and 8 s for UME and ME, respectively.

Method without liquid reagent—the method used was adapted from the one described by Lacombe et al. [11,12], based on the oxidation of a molybdenum wire to form molybdates and protons. Experimentally, molybdenum, reference and working electrodes were placed in a 3 mL compartment. To avoid protons reduction, the counter electrode was isolated from the first compartment by a Nafion® membrane (N117 DuPont™ PFSA). Molybdates and protons were produced with molybdenum anodic oxidation at a constant potential of 0.8 V until a 14.0 C load was reached.

Calibrationless method—successive chronoamperometric measurements were performed *versus* time in semi-infinite diffusion conditions using a gold disk UME and a gold disk ME as working electrodes. For experiments performed with potassium ferrocyanide, a potential of 0.5 V was applied during 60 s on a gold disk UME and during 8 s on a gold disk ME. To analyze the silicomolybdic complex, a potential of 0.34 V was applied during 60 s on a gold disk UME and during 8 s on a gold disk ME.

Technicon Autoanalyser III—the reference colorimetric analysis of silicate was performed according to Tréguer et al.'s method

[35]. Laboratory colorimetric measurements were made with an Auto-Analyzer Technicon III (AAIII, Bran Luebbe). The concentration of the silicate solution, used for the preparation of silicate samples in artificial seawater, was precisely estimated with this technique.

4. Results and discussion

4.1. Electroactive surface determination

As the calibrationless method is very sensitive to the electroactive surface of each electrode (Cottrell's equation in Table 1 with $A_{ME} = \pi r_{ME}^2$ and Eq. (1)), first experiments were carried out to determine the electroactive radius of the working electrodes and check whether the proposed electrochemical equations are suitable. To achieve this, potassium ferricyanide in potassium chloride electrolyte was used as its diffusion coefficient which has been well established (ferricyanide: $D_0 = 6.95 \times 10^{-6}$ cm^2 s^{-1} at 25 °C in 0.2 mol L^{-1} KCl [36]). Three precise fresh solutions of ferricyanide potassium 7.5×10^{-3} mol L^{-1} were prepared in KCl 0.2 mol L^{-1}. Chronoamperometries were achieved on each electrode in semi-infinite conditions (three times for each solution) and the corresponding equations were applied for the disk ME and UME to determine r_{ME} and r_{UME}, respectively.

Knowing the diffusion coefficient D_0, the ferricyanide concentration C_0^* and the corresponding intensity I, the radii r_{ME} and r_{UME} have been calculated. Table 2 shows the comparison between the radius obtained experimentally and the geometrical radius as mentioned by the gold suppliers. The standard deviation obtained for the three determinations on experimental radii is excellent, equal or less than 0.6%. For the commercial electrode (r_{ME}=1.5 mm), the mean value of electroactive radius, determined experimentally, is relatively much closer to the geometric value than for the homemade electrodes with different radii. For the homemade electrodes, observations with an optical microscope revealed an excellent circular shape but deviations concerning the UME radii are slightly more important. Indeed, any deviation of a minute angle of the gold wire from the axis of the electrode body modifies the geometry of the electroactive surface towards an elliptic form instead of a perfect disk. Recent observations done with a Scanning Electronic Microscope have shown that the geometric surface is a well defined disk which makes Eq. 1 perfectly suitable. However, we observed on several UME the presence of a slight porosity. Given the quality of the gold material in our possession, we thus make the hypothesis for the time being that the geometric radius is close enough to the electroactive ones to perform the calibrationless method.

Table 2
Determination of the electroactive radius r_0 of gold disk UME and gold disk ME with precise 7.5×10^{-3} mol L^{-1} potassium ferricyanide solutions in a 0.2 mol L^{-1} KCl electrolyte. Chronoamperometric measurements performed at 0.2 V during 60 s for UME and 8 s for ME.

Geometrical radius	Test 1		Test 2		Test 3	
	r_0	Std dev. r_0 (%)	r_0	Std dev. r_0 (%)	r_0	Std dev. r_0 (%)
r_{UME}=12.5 μm	11.8 μm	0.3	12.5 μm	0.2	13.5 μm	0.3
r_{UME}=25.0 μm	28.5 μm	0.5	29.6 μm	0.2	/	/
rr_{ME}=0.5 mm	0.44 mm	0.4	0.47 mm	0.5	0.48 mm	0.5
r_{ME}=1.5 mm	1.49 mm	0.6	1.51 mm	0.4	1.53 mm	0.3

4.2. Calibrationless method with potassium ferrocyanide

It is proposed here to check the validity of the calibrationless method with the experimental materials used in the laboratory including the homemade UME. For the experiments, potassium ferrocyanide solution has been prepared in a 0.2 mol L^{-1} KCl electrolyte. The use of this compound presents a double interest as verification can be done on one hand on the diffusion coefficient, already estimated in a former study (ferrocyanide: $D_0 = 6.12 \times 10^{-6}$ cm^2 s^{-1} at 25 °C in 0.2 mol L^{-1} KCl [36]), and on the other hand on the concentration prepared accurately from potassium ferrocyanide salt.

The solution was prepared with argon bubbling to preserve ferrocyanide from oxidation. During the measurement, argon atmosphere was kept over the solution with a slow flux to avoid any stirring of the liquid, and to preserve the experimental semi-infinite diffusion conditions.

Chronoamperometry was successively applied on each electrode, and Cottrell's equation (Table 1) and Eq. (1) mentioned previously were used to estimate both diffusion coefficient D_0 and concentration of ferrocyanide C_0^*. Some tests were done for different concentrations of ferrocyanide on a couple of electrodes of radii 25.0 μm for UME and 1.5 mm for ME. As proposed in Section 4.1, geometrical radii were used for the calculations. The results are summarized in Table 3 and compared to the diffusion coefficient of ferrocyanide found by Bortels et al. [36] and the known concentration.

As it can be noticed in Table 3, the results are in good agreement with the diffusion coefficient value from literature. The repeatability of the measurement in the same solution is particularly good to determine a constant diffusion coefficient value. The concentration of ferrocyanide determined experimentally is also very close to the known value. These results give us some confidence in applying this calibrationless method for silicate determination.

4.3. Calibrationless method with silicate

Previous studies of the silicomolybdic complex by cyclic voltammetry have shown two successive and reversible reduction

Table 3
Calibrationless method applied for the determination of ferrocyanide diffusion coefficient and its standard deviation (%) from the data obtained in the literature [36]. Chronoamperometric measurements performed at 0.5 V in 10 mL of potassium ferrocyanide solutions at different concentrations in a 0.2 mol L^{-1} KCl electrolyte.

r_{UME} (μm)	r_{ME} (mm)	D_0 ferrocyanide (10^{-6} cm^2 s^{-1})	% Error D_0	C_0^* known ferrocyanide (10^{-3} mol L^{-1})	C_0^* experimental ferrocyanide (10^{-3} mol L^{-1})	Error=$\frac{C_0^* exp - C_0^* known}{C_0^* known}$ (in %)
12.5	1.5	6.16	0.7	3.45	3.43	−0.6
12.5	1.5	6.13	0.2	3.45	3.44	−0.3
12.5	1.5	6.14	0.3	5.21	5.16	−1.1
12.5	1.5	5.97	2.5	5.21	5.16	−1.1
12.5	1.5	6.36	3.9	7.32	7.17	−2.0
12.5	1.5	6.24	2.0	7.32	7.11	−2.9

waves involving two and three electrons transfer, respectively [9–12]. In the present study, results obtained come from the first reduction step of the silicomolybdic complex. Chronoamperometry was used with a potential applied at 0.34 V. Linearity was noticed between the current intensity and the concentration of the silicomolybdic complex for transient and steady states on ME and UME, respectively. For this reason the diffusion coefficient value is considered to be independent of the range of concentrations considered.

Silicate concentration was determined from the silicomolybdic complex with a reagentless method. A volume of 3 mL of a silicate solution was prepared in artificial seawater and introduced in the measurement cell. In the same compartment, a molybdenum electrode was placed with the reference and working gold ME and UME. The counter electrode was separated from the cell by a Nafion® membrane to avoid reduction of protons. This technical solution is also an advantage for the future development of an *in situ* sensor as the formation of gas in the measurement cell is prohibited. The molybdenum electrode was oxidized at 0.8 V until 14.0 C were reached, this charge was experimentally determined to obtain a pH lower than 1.5. During the oxidation of molybdenum, a black oxide layer covered the surface of the material, but this phenomenon did not affect the formation of molybdates and the achieved pH value. Indeed, some reproducibility tests, done on 10 oxidations of molybdenum, allowed reaching a pH value of 1.43 ± 0.02 and a reproducible current intensity measured for the reduction of the silicomolybdic complex (less than 3 standard deviations for 5 current intensity measurements of silicate concentration of 8.6×10^{-6} mol L^{-1}).

In the cell where molybdenum was oxidized, complexation of silicate with molybdates was carried out during 6 min under stirring, forming the electroactive Keggin anion $H_4Si(Mo_{12}O_{40})$ described in details by Lacombe et al. [11,12]:

$$Si(OH)_4 + 12MoO_4^{2-} + 24H^+ \rightarrow H_4Si(Mo_{12}O_{40}) + 12H_2O$$

Successive chronoamperometric measurements of current *versus* time have been performed using a pair of gold disk electrodes of 12.5 or 25.0 μm radii for the UME and 1.0 or 1.5 mm radii for the ME. As good results were obtained with the calibrationless method applied to ferrocyanide, no prior determination of the electroactive surface was done before silicate determination and geometrical radii were used for the calculations. The potential was imposed during 8 s on the ME and during 60 s on the UME. Current as function of time (Fig. 2a) and steady-state current (Fig. 2b) have been used to calculate first the diffusion coefficient D_0 of the silicomolybdic complex with Eq. (2) and using the different radii values for the different pairs of electrodes.

Even if the method allows a theoretical detection of silicate, some characteristics of the voltammograms were verified systematically to apply the equations in correct conditions. Experimentally, the absence of stirring makes possible the hypothesis of semi-infinite conditions for the diffusion. Concerning data collected from the ME, the current intensity was systematically plotted *versus* $t^{-1/2}$ to verify the linearity of the correlation for times between 0.1 and 8 s, as shown in Fig. 2. This linearity shows that our experimental conditions respect Cottrell's equation (Table 1) and that the current is controlled by diffusion-controlled mass transport. To be sure to avoid both effects of double layer discharge at shorter times and limitation due to natural convection at longer times, we kept a range between 1 and 3 s for our calculations. For the UME, as time to achieve steady state current depends on several parameters [37], an experimental time of 30 s appeared sufficient to achieve steady state with a constant current intensity for a gold disk UME of 25 μm radius.

Different concentrations of silicate have been prepared from 55 to 140×10^{-6} mol L^{-1} in artificial seawater. The results obtained are reported in Table 4. The average value obtained for the diffusion coefficient of the silicomolybdic complex is $2.2 \pm 0.4 \times 10^{-6}$ cm^2 s^{-1} which is consistent with diffusion coefficient values of molecules in liquid media. Concerning the concentration, good results were observed when comparing known concentrations of silicate with experimentally derived concentrations. It must be noticed that the lowest deviation to known concentrations concerns the pair of electrodes of 12.5 μm and 1.5 mm radii for UME and ME, respectively. This can be explained by the fact that mass transfer behavior in these conditions is closer to the corresponding Cottrell's equation and Eq. (1) for ME and UME, respectively. Indeed, on one hand spherical diffusion is more predominant when the radius of the electrode is smaller and on the other hand perpendicular diffusion is much present for ME with a large surface. However, as compared to the excellent results with potassium ferrocyanide in Section 4.2, those obtained with silicate are less accurate. The main difference is the range of concentrations of silicate shifted towards lower concentrations as compared with potassium ferrocyanide. In these conditions, the required precision for the electroactive surfaces of both ME and UME becomes essential and the even slight presence of porosity might be an issue.

Starting from these results, further work is under progress with smaller radii for the UME and the use of gold from another supplier certifying the absence of porosity. As the size of the UME will be reduced, the main difficulty will be to acquire a current intensity under a few pico-amperes as noise will become predominant at this measurement scale. To get around this difficulty

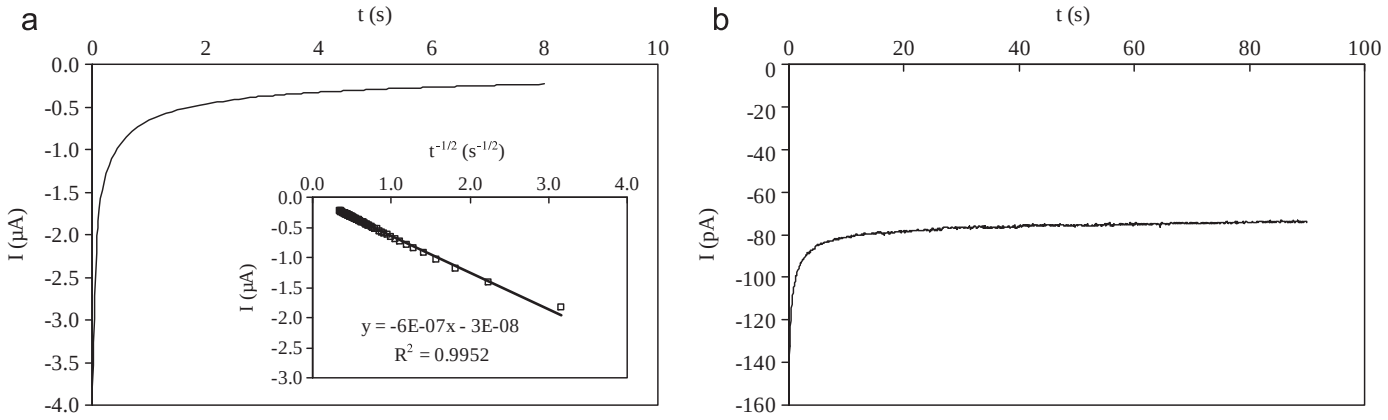

Fig. 2. Chronoamperograms performed at 0.34 V in 57.1×10^{-6} mol L^{-1} silicate in artificial seawater. (a) Reduction time of 8 s on the 1.5 mm radius gold ME. Regression of current intensity *vs* $t^{-1/2}$ plot for reduction of silicomolybdic complex in the range 0.1–8 s. (b) Reduction time of 60 s on the 25.0 μm gold disk UME.

Table 4
Calibrationless method applied for the determination of diffusion coefficient of silicomolybdic complex and concentration of silicate solutions prepared at different concentrations in artificial seawater. Amperometric measurements performed at 0.34 V in a volume of 3 mL of solution after oxidation of molybdate at 0.8 V to reach 14.0 C.

r_{UME} (μm)	r_{ME} (mm)	D_0 silicomolybdic complex (10^{-6} cm^2 s^{-1})	C_0^* known silicate (10^{-6} mol L^{-1})	C_0^* experimental silicate (10^{-6} mol L^{-1})	Error$=\frac{C_0^* exp - C_0^* known}{C_0^* known}$ (in %)
25.0	0.5	1.4	55.2	52.4	−5.1
12.5	1.5	2.2	57.1	56.6	−0.9
12.5	1.5	2.4	107.3	107.3	0.0
12.5	0.5	1.9	139.7	152	8.8
25.0	0.5	2.3	139.7	136	−2.6
25.0	1.5	2.5	139.7	153.6	9.9
12.5	0.5	2.6	139.7	135.0	−3.4

some UME-arrays will be used that will allow the acquisition of a more acceptable signal and the increase of the signal to noise ratio. Building micro-devices with gold electrodes obtained by Chemical Vapor Deposition (CVD), where surface roughness of the electrode is highly reduced and its geometry accurately controlled, is the way forward to achieve perfect smooth surfaces. This process will allow us to obtain mass-produced electrodes (ME and UME) with miniaturized systems.

With a suitable protocol to electrochemically clean the electrode, reproducible results with a wider range of silicate concentrations ($0.1–140.0 \times 10^{-6}$ mol L^{-1}) are foreseen with our calibrationless method. This is the next step towards ANESIS, our Autonomous Nutrients Electrochemical Sensor *in situ* for silicate detection.

Acknowledgments

William Giraud and Ludovic Lesven were supported by the Foundation STAE (Sciences and Technologies for Space and Aeronautics) within the project "MAISOE" (Microlaboratories of *in situ* Analyses for Environmental Observatories). Carole Barus was supported by INSU funding and Justyna Jońca was supported by Marie Curie Ph.D. Grant within the SENSEnet ITN (EC Framework Programme 7, Grant Agreement no. 237868).

References

[1] D.J. Conley, Limnol. Oceanogr. 42 (1997) 774–777.
[2] D.J. Conley, P. Stålnacke, H. Pitkänen, A. Wilander, Limnol. Oceanogr. 45 (2000) 1850–1853.
[3] V. Smetacek, Nature 391 (1998) 224–225.
[4] A.C. Redfield, B.H. Ketchum, F.A. Richards, in: M. N. Hill (Ed.), The Composition of Sea-Water Comparative and Descriptive Oceanography, Interscience Pub, New York: 1963, pp. 26–77.
[5] P. Tréguer, P. Pondaven, Nature 406 (2000) 358–359.
[6] P. Tréguer, P. Le Corre, Manuel d'analyse des sels nutritifs dans l'eau de mer (Utilisation de l'autoanalyser II Technicon), 2nd edition, Université de Bretagne occidentale, France, 1975.
[7] L. Hua-Bin, F. Chen, J. Chromatogr. A 874 (2000) 143–147.
[8] D. Thouron, R. Vuillemin, X. Philippon, A. Lourenco, C. Provost, A. Cruzado, V. Garcon, Anal. Chem. 75 (2003) 2601–2609.
[9] N.G. Carpenter, A.W.E. Hodgson, D. Pletcher, Electroanalysis 9 (1997) 1311–1317.
[10] A.W.E. Hodgson, D. Pletcher, Electroanalysis 10 (1998) 321–325.
[11] M. Lacombe, V. Garçon, M. Comtat, L. Oriol, J. Sudre, D. Thouron, N. Le Bris, C. Provost, Mar. Chem. 106 (2007) 489–497.
[12] M. Lacombe, V. Garçon, D. Thouron, N. Le Bris, M. Comtat, Talanta 77 (2008) 744–750.
[13] J. Jońca, V. León Fernández, D. Thouron, A. Paulmier, M. Graco, V. Garçon, Talanta 87 (2011) 161–167.
[14] A.J. Bard, L.R. Faulkner, Electrochemical Methods: Fundamentals and Applications, second ed., Wiley, New York, 2000.
[15] B.J. Feldman, S.W. Feldberg, R.W. Murray, J. Phys. Chem. 91 (1987) 6558–6560.
[16] M. Mosbach, T. Laurell, J. Nilsson, E. Csöregi, W. Schuhmann, Anal. Chem. 73 (2001) 2468–2475.
[17] S. Licht, V. Cammarata, M.S. Wrighton, J. Phys. Chem. 94 (1990) 6133–6140.
[18] C. Amatore, C. Sella, L. Thouin, J. Electroanal. Chem. 593 (2006) 194–202.
[19] E. Beinrohr, M. Cakrt, J. Dzurov, L. Jurica, J.A.C. Broekaert, Electroanalysis 11 (1999) 1137–1144.
[20] E. Beinrohr, Accred. Qual. Assur. 6 (2001) 321–324.
[21] P.J. Lingane, Anal. Chem. 36 (1964) 1723–1726.
[22] C. Amatore, M. Azzabi, P. Calas, A. Jutand, C. Lefrou, Y. Rollin, J. Electroanal. Chem. 288 (1990) 45–63.
[23] M. Tsushima, K. Tokuda, T. Ohsaka, Anal. Chem. 66 (1994) 4551–4556.
[24] C. Biondi, L. Bellugi, J. Electroanal. Chem. 24 (1970) 263–270.
[25] J.J. Lingane, B.A. Loveridge, J. Am. Chem. Soc. 72 (1950) 438–441.
[26] O.R. Brown, J. Electroanal. Chem. 34 (1972) 419–423.
[27] M. Kakihana, H. Ikeuchi, G.P. Satô, K. Tokuda, J. Electroanal. Chem. 117 (1981) 201–211.
[28] P.C. Winlove, K.H. Parker, R.K.C. Oxenham, J. Electroanal. Chem. 170 (1984) 293–304.
[29] G. Denuault, M.V. Mirkin, A.J. Bard, J. Electroanal. Chem. 308 (1991) 27–38.
[30] D. Bustin, Š. Mesároš, M. Rievaj, P. Tomčík, Electroanalysis 7 (1995) 329–332.
[31] D. Menshykau, A.M. O'Mahony, M. Cortina-Puig, F.J. del Campo, F.X. Muñoz, R.G. Compton, J. Electroanal. Chem. 647 (2010) 20–28.
[32] P. Jenčušová, P. Tomčík, D. Bustin, M. Rievaj, Z. Dovalovská, Chem. Pap. 60 (2006) 173–178.
[33] C. Amatore, S. Szunerits, L. Thouin, J.S. Warkocz, J. Electroanal. Chem. 500 (2001) 62–70.
[34] C. Amatore, C. Pebay, L. Thouin, A. Wang, J.S. Warkocz, Anal. Chem. 82 (2010) 6933–6939.
[35] P. Tréguer, P. Le Corre, P. Courtot, J. Cons. Int. Explor. Mer 36 (1976) 289–294.
[36] L. Bortels, B. Van den Bossche, J. Deconinck, S. Vandeputte, A. Hubin, J. Electroanal. Chem. 429 (1997) 139–155.
[37] C. Amatore, C. Pebay, L. Thouin, A. Wang, J.S. Warkocz, Anal. Chem. 82 (2010) 6933–6939.